J Fluoresc (2012) 22:639–649
DOI 10.1007/s10895-011-1000-6

ORIGINAL PAPER

Synthesis of Novel Eu(III) Luminescent Probe Based on 9- Acridinecarboxylic Acid Skelton for Sensing of ds-DNA

Hassan A. Azab · Belal H. M. Hussein · Abdullah I. El-Falouji

Received: 9 July 2011 / Accepted: 14 October 2011 / Published online: 9 November 2011

Abstract Eu(III)-9-acridinecarboxylate (9-ACA) complex was synthesized and characterized by elemental analysis, conductivity measurement, IR spectroscopy, thermal analysis, mass spectroscopy, ^{1}H-NMR, fluorescence and ultraviolet spectra. The results indicated that the composition of this complex is [Eu(III)-(9-ACA)$_2$(NCS)(C_2H_5OH)$_2$] 2.5 H_2O and the oxygen of the carbonyl group coordinated to Eu(III). The interaction between the complex with nucleotides guanosine 5′- monophosphate (5′-GMP), adenosine 5′-diphosphates (5′-ADP), inosine (5′-IMP) and CT-DNA was studied by fluorescence spectroscopy. The fluorescence intensity of Eu(III)-9-acridinecarboxylate complex was enhanced with the addition of CT-DNA. The effect of pH values on the fluorescence intensity of Eu(III) complex was investigated. Under experimental conditions, the linear range was 9–50 ng mL^{-1} for calf thymus DNA (CT- DNA) and the corresponding detection limit was 5 ng mL^{-1}. The results showed that Eu (III)-(9-ACA)$_2$ complex binds to CT-DNA with stability constant of 2.41×10^4 M .

Keywords Eu(III)-9-acridinecarboxylate · Luminescent probe · ds- DNA · Nucleotides

H. A. Azab (✉) · B. H. M. Hussein
Chemistry Department, Faculty of Science,
Suez Canal University,
Ismailia 41522, Egypt
e-mail: azab2@yahoo.com

A. I. El-Falouji
Biotechnology Research Center, Suez Canal University,
Ismailia 41522, Egypt

Introduction

DNA plays an important role in the life process because it contains the genetic information related to cellular function. The interaction of DNA with small molecular compounds has great importance to understand the reaction mechanisms of some anti-tumor, anti-viral drugs and to design new DNA-targeted drugs. Currently, a lot of studies report complexes of rare earth ions possess an antitumor activity [1, 2]. In order to develop new antitumor drugs, which specifically target DNA, it is necessary to understand the different binding modes. Basically, metal complexes interact with the double helical DNA in either a non-covalent or a covalent way. A number of techniques have been employed to study the interaction of drugs with DNA [3–8], including fluorescence spectroscopy [9], UVspectrophotometry [10], electrophoresis [11], nuclear magnetic resonance [12], and electrochemical methods [13]. In recent years, there is a growing interest in the absorption and fluorescence investigations of interactions between anticancer drugs and other DNA targeted molecules and DNA [14–16]. UV–vis absorption and fluorescence spectroscopy are regarded as effective methods among these techniques because they are sensitive, rapid and simple [17]. The interaction of fluorescent metal complexes containing multidentate aromatic ligands with DNA has gained much attention. This is due to their possible application as new therapeutic agents and their attractive emission properties such as long lifetime; large Stokes' shift, and line like emission, which make them potential probes of DNA structure and its conformation [7, 18]. Acridines have

been a topic of interest for a long time owing to their biological activities, numerous applications and the ability to intercalate tightly to DNA helical structure [3]. Acridine derivatives have found diverse usage such as antimalarial [5], antiprotozoal [6], antibacterial [7] and anticancer drugs [8, 14]. Owing to the high fluorescence quantum yield and large binding constants to DNA [15], acridine derivatives are well known in the field of development of probes for nucleic acid structure and conformational determination [19–21]. In this work, we used UV–vis absorption and fluorescence spectroscopy to explore the interaction between Eu(III)-(9-ACA)$_2$ complex and calf thymus DNA. We believe this will be helpful to further understand the mechanism of interactions between DNA and acridine's rare earth metal complexes as well as further understand acridine's pharmacological effects. The knowledge gained from this study should be useful for the development of potential probes for DNA structure and new therapeutic reagents for tumors. This work is a continuation for the author's work in the field of developing new luminescent probes [22–29].

Experimental

Chemicals

9-Acridinecarboxylic acid, $EuCl_3 \cdot 6H_2O$, adenosine 5′-diphosphates (5′-ADP), guanosine 5′-monohosphates (5′-GMP), and inosine 5′-monohosphate (5′-IMP) were purchased from Sigma. Calf thymus DNA (CT-DNA) was obtained from Sigma-Aldrich Biotech. Co., Ltd. They were used without purification. The purity of CT-DNA was checked by monitoring the ratio of absorbance at 260 to 280 nm. The ratio was 1.89, indicating that the CT-DNA was free from protein [30].

Stock Solutions

Deionized double-distilled water and analytical grade reagents were used throughout. CT-DNA stock solution was prepared by dissolving the solid material in aqueous tris-buffers (pH 7.2). The concentration of the CT-DNA stock solution was determined by nanodrop absorption spectrophotometer ND-1000 using the molar absorption coefficient (6,600 M^{-1} cm^{-1}) at 260 nm [31]. CT-DNA solutions were stored at 4 °C for more than 24 h with gentle shaking occasionally to get homogeneity and used within 2 days. The concentrations of the metal ion stock solutions were determined complexometrically by ethylenediamine tetracetic acid dissodium salt (EDTA) using suitable indicators [32].

Measurements

Fluorescence spectra were recorded with Jasco-6300 spectrofluorometer equipped with a 150 W xenon lamp source and quartz cells of 1 cm path length. The slit widths for excitation and emission were set to 5.0 and 5.0 nm, respectively. All data and each spectrum were the 5 nm/5 nm. All absorption spectra were performed on a Perkin-elmer lambda 25 UV–vis spectrophotometer equipped with quartz cells. The pH values were adjusted by using Fisher account pH/ion meter model/825 MP. Elemental analysis was carried out by Elementar vario; thermogravimetric analysis was carried out by (a Shimazdu TGDTG).^{1}H NMR spectra were performed with Varian UNITY-500 instrument; the infrared spectra were obtained in the 4,000–500 cm^{-1} region by using Bruker Alpha with KBr discs. Melting point was determined on a MEL-TEMP II apparatus (thermometer uncorrected). The fluorescence spectra and intensities were monitored at the fixed analytical emission wavelength (λem=615 nm) of the complex in DMSO solution. Fluorescence titrations were performed in a 1 cm quartz cuvette by successive addition of DNA (1.35×10^{-6}–3×10^{-5} M) to solutions of 1.0×10^{-5} M Eu(III)-(9-ACA)$_2$ complex. Before reacting Eu(III) complex with CT-DNA, its solution behavior in buffer solutions at room temperature was monitored by UV–vis and fluorescence measurements for 24 h. Liberation of the ligand was not observed under these conditions. These suggest that the complex is stable under our experimental conditions. The titration data was analyzed according to modified Stern-Volmer equation to investigate the types of interaction of Eu(III)-(9-ACA)$_2$ complex with different DNA concentrations.

Synthesis of Eu(III)-(9-ACA)$_2$ Complex

The complex was synthesized by a method similar to that reported by Hart and Laming [33]. $EuCl_3 \cdot 6H2O$ (1.35×10^{-3} mol) dissolved in 25 cm^3 ethanol was treated with a solution of potassium thiocyanate (5.40×10^{-3} mol) in 75 cm^3 ethanol in 1:4 molar ratio. The two solutions were mixed thoroughly and the precipitate of potassium chloride was removed by filtration. The filtrate was added slowly with vigorous stirring to a solution of (9-acridinecarboxylic acid) (5.40×10^{-3} mol) in 50 cm^3ethanol (1: 4 molar ratio). Precipitate appeared immediately after mixing the two solutions and raising the pH to 7.5. Stirring overnight for 24 h to complete precipitation has been performed. This product was collected by filtration, purified by washing several times with ethanol and dried in vacuum over P_4O_{10}.

Results and Discussion

Characterization of the Eu(III)-(9-ACA)$_2$ Complex

Elemental Analysis and Conductivity Measurement

Analytical data for the synthesized Eu(III)-(9-ACA)$_2$ complex is presented in Table 1. The elemental analytical data show that the formulas of the complex may be [Eu (9-ACA)$_2$(NCS)(C_2 $H_5OH)_2$] 2.5H_2O as indicated in (Fig. 1). The complex is brown colored and stable. It is soluble in DMF and DMSO and insoluble in water, ethanol, benzene, diethyl ether and tetrahydrofuran. Because of the insolubility of the complex in suitable solvents we were unsuccessful in growing crystals for single crystal X-ray structural studies. The molar conductance measurement of the Eu(III)-complex was performed in DMSO solution (with concentration of 1×10^{-4} M) at room temperature. The value of molar conductance is 13 Sm^2mol^{-1}, indicating that the complex is a nonelectrolyte.

Thermal Analysis

The thermal decomposition of the Eu(III)-(9-ACA)$_2$ complex was studied using the thermogravimetric (TG) and differential thermal gravimetry (DTG) techniques as shown in (Fig. 2). The experiment was performed under N_2 atmosphere with a heating rate of 10 °C/min in the temperature range of 25–800 °C. The TG curve exhibits many steps of weight losses. The first mass loss is due to dehydration with loss of non-coordinating water (2.5H_2O; calculated=5.01%; TG=5.22%). The release of water was accompanied by an endothermic effect on the DTG curve observed at 53.3 °C. The second weight loss peak occurred at 220 °C corresponding to endothermic peak due to the removal of thiocyanate (calculated=8.01%; TG=8.22%). The third significant weight loss of 50.1% occurred from 350 to 520 °C corresponding to the decarboxylation and decomposition of 9-ACA ligand (calculated: 52.37%; TG=53.52%). The decomposition of the organic moiety was reflected by strong endothermic effect on DTG curve with the maximum at 497.8 °C. The remaining weight of 24.84% corresponds to the percentage (26.95%) of Eu and O components, indicating that the final thermal decomposition residue is Eu_2O_3.

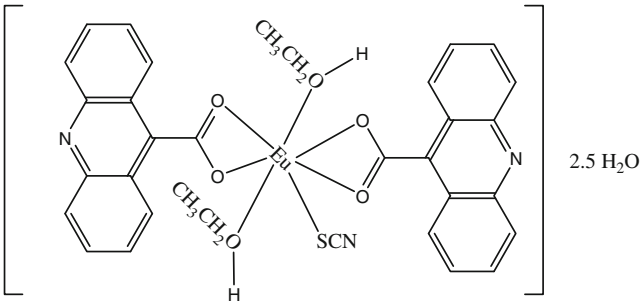

Fig. 1 Suggested structure of Eu (III)-(9-ACA)$_2$ complex

Infrared Spectra

The IR spectral data of the ligand and its Eu(III) complex were depicted in (Fig. 3). In the IR spectra of the ligand 9-ACA, weak bands were observed at 3,445 cm^{-1} which can be attributed to the OH group. In addition, the high intensity sharp bands at 1,651 and 1,608 cm^{-1} were assigned to C=O and C=C groups, respectively. The band at 1,608 cm^{-1} confirms the presence of the aromatic ring.

The Eu(III) complex exhibited broad weak intensity band at about 3,370 cm^{-1}, which was assigned to crystal water and the coordinated ethanol molecule [34]. The high intensity band appearing around 1,651 cm^{-1} in 9-ACA which was ascribed to C=O, downshifted to 1,563 cm^{-1} in the Eu(III) complex, this confirms that the oxygen atoms of C=O coordinated to Eu(III) ions successfully. In the IR spectra of the complex, the characteristic bands of the carboxylate groups appeared at 1,571 cm^{-1} for the antisymmetric stretching vibrations, $\nu_{as}(COO^-)$ and at 1,384 cm^{-1} for the symmetric stretching vibrations, $\nu_s(COO^-)$, respectively. The separation ($\Delta\nu$) between $\nu_{as}(COO^-)$ and $\nu s(COO^-)$ is 187 cm^{-1}, indicating bidentate coordination of the carboxylate groups in such complexes [35, 36]. It was observed that the characteristic absorption peak of the thiocyanate (NCS) was at about 2,051 cm^{-1} [37]. The complex showed medium intensity bands in the region 413 cm^{-1} which was assigned to EuO modes. According to the results above, the ligand coordinated to the Eu(III) ions via the oxygen atoms of the carbonyl, and hydroxyl groups.

Table 1 Elemental analytical data for the Eu(III)-9-ACA complex

Complex	C(%) found (calc.)	H (%) found (calc.)	N (%) found (calc.)	Eu (%) found (calc.)
[Eu (9-ACA)$_2$(SCN)($C_2H_5OH)_2$] 2.5H_2O	50.79 (50.1)	4.04 (3.44)	4.7 (5.3)	20.01 (19.21)

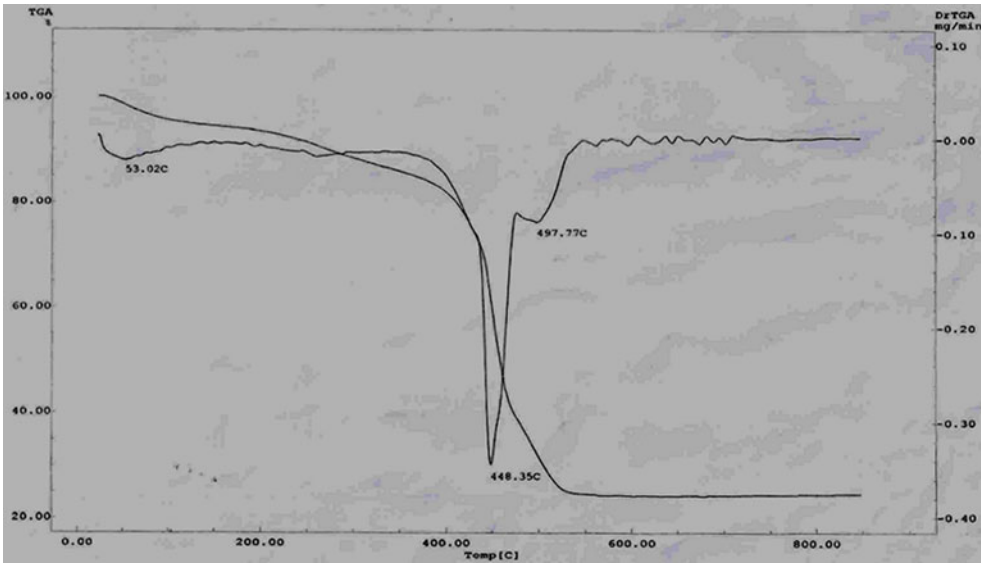

Fig. 2 TG and DTA curves of Eu(III) complex

Mass Spectroscopic Studies

The molecular ion peak (M^+.) is observed at m/z 791, which is ascribed to [Eu(9-ACA)$_2$(NCS) ($C_2H_5OH)_2$] 2.5H_2O coinciding with the calculated value (791.26). In addition to this the fragment ion peaks observed at m/z equals 733 and 653 are due to M-NCS, and M-(2EtOH$^+$2.5 H_2O), respectively. Since m/z 791 is an odd number, there are odd nitrogen atoms present (3 nitrogen atoms).

^{1}H NMR Spectra

The ^{1}H NMR spectra of 9-ACA and its Eu(III) complex were measured and analyzed to confirm the complex formation. The chemical shifts of the ^{1}H NMR spectra in DMSO-d^6 were presented as follows: 9-ACA ($C_{10}H_6O_4$): ^{1}H NMR (DMSO-d^6): 8.68 (H4), 7.83 (H5), 7.67 (H7), 7.38 (H8), 7.32 (H6); Eu(9-ACA)$_2$(SCN)(EtOH)$_2$: ^{1}H NMR (DMSO-d^6): 8.53 (H4), 7.70 (H5), 7.57 (H7), 7.24(H8), 7.19 (H6). A survey of the spectral data reveals downfield chemical shifts of the protons in the Eu(III) complex spectrum relative to the free ligand. The carboxylic proton peak is absent in the spectrum of the complex due to the deprotonation of the carboxylic group. On the basis of the elemental analysis, thermal decomposition, IR, ^{1}H NMR and mass spectra, the suggested structure of the complex is consistent with that shown in (Fig. 1).

Steady State Uv-Visible Absorption and Fluorescence Spectra of Eu(III) –(9-ACA)$_2$

The absorption spectra of 9-ACA and Eu(III)-(9-ACA)$_2$-complex have been investigated in DMSO as shown in

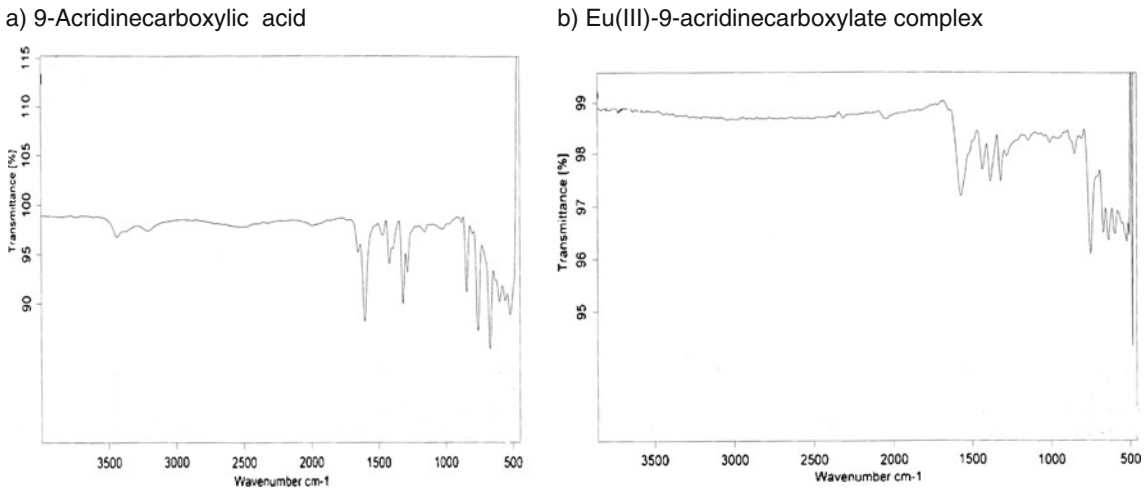

Fig. 3 The IR spectra of **a** ligand and **b** Eu(III) complex

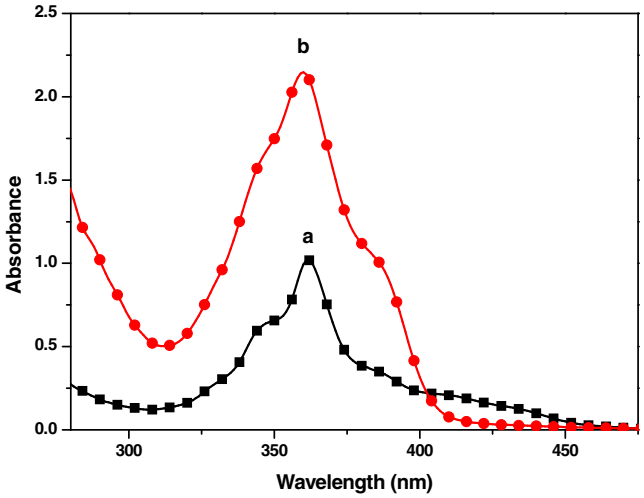

Fig. 4 UV absorption spectra of **a** 9-ACA and **b** Eu(III)-(9-ACA)$_2$ complex. Conditions: in DMSO, 25 °C, 9-ACA at 2×10^{-5} M, Eu(III)-(9-ACA)$_2$ at 2×10^{-5} M

(Fig. 4). 9-ACA exhibits an absorption band with a maximum at 361 nm, while its complex with Eu(III) ion was slightly blue shifted to 357 nm with higher extinction coefficient than that of 9-ACA. The fluorescence spectrum of Eu(III)-(9-ACA)$_2$ complex shown in (Fig. 5) was measured in DMSO at room temperature . The spectrum of 9-ACA and its Eu-complex exhibits two peaks at 413 and 432 nm. Fluorescence spectrum of Eu(III)-(9-ACA)$_2$ complex shows the characteristic emission bands for Eu (III) ions [38]. The emission band centered at 615 nm ($^5D_0\rightarrow{}^7F_2$) is obviously higher than the other emission bands at 590 nm ($^5D_0\rightarrow{}^7F_1$), 645 nm ($^5D_0\rightarrow{}^7F_3$), and 690 nm ($^5D_0\rightarrow{}^7F_4$), respectively.

The fluorescence spectra of Eu(III)-(9-ACA)$_2$ in DMSO containing various percentages of water have been measured. Figure 6 shows that the fluorescence intensity increases with an increase in the percentage of water in DMSO in the region of ligand emission (413 and 432 nm). The increase of fluorescence quantum yield of many heterocyclic organic molecules, e.g., quinoline and isoquinoline including acridine, in protic solvents is reported in the literature [39, 40]. On the other hand the fluorescence intensity of Eu(III) increases with increasing the water content passing through a maximum at 30% water content. The characteristic emission bands of Eu (III) were completely quenched above 60% water content.

Interaction of Eu(III)-(9-ACA)$_2$ Complex with Different Nucleotides and CT-DNA

Fluorescence Studies

The interaction of Eu(III)-(9-ACA)$_2$ with CT-DNA, 5′-GMP, 5′-IMP and 5′-ADP in Tris–HCl buffer of pH 7.4 has been investigated by fluorescence measurement as shown in (Fig. 7). The addition of nucleotides and DNA enhances the emission bands of Eu(III)-(9-ACA)$_2$ complex through the intramolecular energy transfer from the exited states of the ligands. On the other hand, CT-DNA and 5′-GMP strongly quenched the fluorescence intensity of ligand band in Eu(III)-complex, while 5′-ADP slightly enhanced the fluoresce intensity of ligand. The ratio of the relative fluorescence intensity I_f/I_0 values which were determined from the ratio of maximum fluorescence intensity in presence and in absence of nucleotide or DNA were listed in Table 2. The higher values for fluorescence enhancement for Eu(III) band have been observed in the presence of CT-DNA and 5′-ADP.

Effect of pH on the Fluorescence Intensity

The luminescence intensity of Eu(III)-(9-ACA)$_2$-DNA system is strongly dependent on pH values as shown in (Figs. 8 and 9). The maximum luminescence intensity of the system is reached at pH 7.4. Therefore, we choose pH 7.4 (0.1 M Tris – HCl buffer) for further experimental studies .The maximum emission intensity of the complex has been observed at 434 nm in the pH range 7.4–11.0, while the broad bands at 456 and 474 nm have been recorded at pH 3.0 as shown in (Figs. 8 and 9).

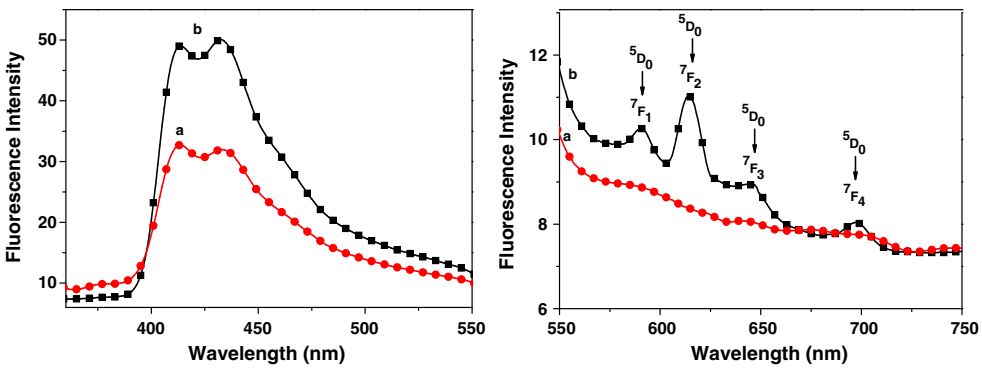

Fig. 5 Fluorescence emission spectra of **a** 9-ACA and **b** Eu (III)-(9-ACA)$_2$ complex Conditions: in DMSO, 25 °C, 9-ACA at 2×10^{-5} M, Eu(III)-(9-ACA)$_2$ at 2×10^{-5} M, λ_{ex}=290 nm

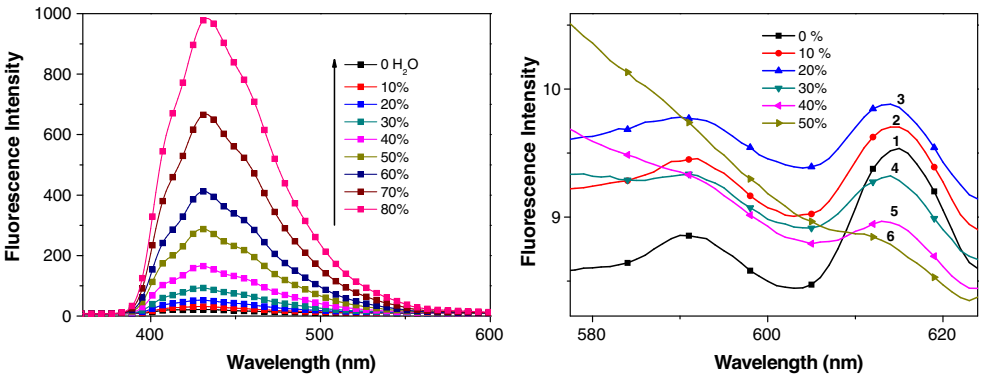

Fig. 6 Effect of water percentage on intensity of fluorescence spectra of Eu(III)-(9-ACA)$_2$ complex in DMSO at λ_{ex}=290 nm

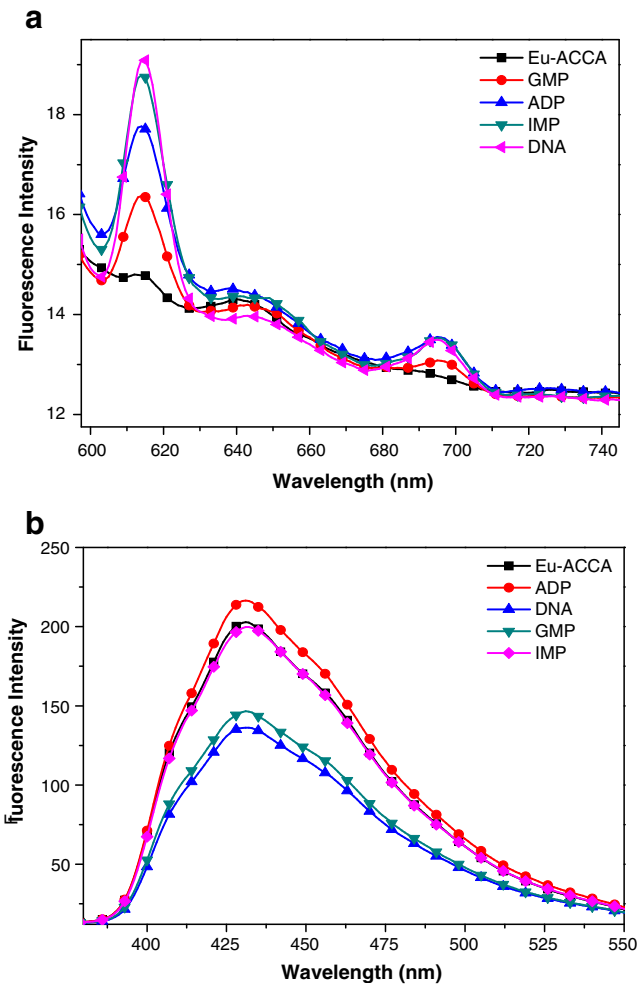

Fig. 7 The fluorescence intensity of Eu (III)-(9-ACA)$_2$ complex in the absence and in the presence of **a** DNA, **b**Nucleotides. Conditions: in Tris–HCl buffer pH 7.4, 25 °C, 9-ACA at 2×10^{-5} M, Eu(III)-(9-ACA)$_2$ at 2×10^{-5} M, λ_{ex}=290 nm, Emission and excitation slit width were 5 nm

Effect of DNA Concentration on Eu(III)-(9-ACA)$_2$ Complex

UV–vis Absorption Spectra

Electronic absorption spectroscopy is employed to identify the binding mode of DNA with metal complexes. Three fundamentally different modes of DNA binding by metal complex can be identified: non-specific external association, groove binding in which the small molecules bound to nucleic acids are located in the major or minor groove [41]. Long-range assembly on the molecular surfaces of nucleic acids has been also observed so that the small molecules are not related to the groove structure of the nucleic acids [1]. Among these interactions, the intercalative binding is stronger than other two binding modes because the surface of intercalative molecule is sandwiched between the aromatic, heterocyclic base pairs of DNA [42]. It was reported that the intercalating ability increases with the planarity of ligands [43, 44]. The absorption spectra of the 9-ACA and its complexes in absence and presence of DNA are given in (Fig. 10). The increase of DNA concentration resulted in clear hyperchromicity in the absorption spectra at the maximum absorbance with a slight blue shift from 358 to 355 nm. The hyperchromicity in π-π* transition and the blue shift in the absorption spectra of Eu(III)-9-ACA complex indicated the formation of some sort of binding most probably groove binding between the Eu(III)-(9-ACA)$_2$ complex and DNA and involves a staking interac-

Table 2 I_f/I_0 ratio for the Eu(III)-(9-ACA)$_2$ complex in the presence and absence of DNA or nucleotides

Compounds	I_f/I_0 (613 nm)	I_f/I_0 (431 nm)
Eu(III)-(9-ACA)$_2$-DNA	1.29	0.67
Eu(III)-(9-ACA)$_2$-ADP	1.27	1.1
Eu(III)-(9-ACA)$_2$-GMP	1.2	0.72
Eu(III)-(9-ACA)$_2$-IMP	1.11	0.98

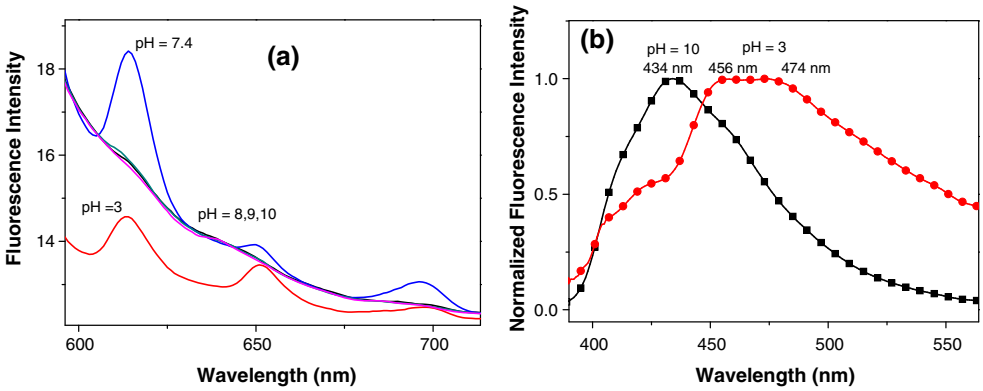

Fig. 8 Fluorescence spectra of Eu(III)-(9-ACA)$_2$ complex in the presence of DNA at different pH values

tion between the aromatic chromophore and the base pairs of DNA i.e. these changes are typical of complexes bound to DNA through non covalent interaction [45]. Hyperchromism may result from the secondary damage of DNA double helix structure [46].

The association constant of the formed complex (K) between the Eu-complex and DNA is given by a Benesi-Hildebrand plot [47].

$$\frac{1}{\Delta A} = \frac{1}{[Eu-complex]_0}\left(\frac{1}{\Delta\varepsilon} + \frac{1}{K\,[DNA]_0\,\Delta\varepsilon}\right) \quad (1)$$

Where ΔA is the difference between the absorbance of Eu-complex in the presence and in the absence of DNA, Δε the difference between the molar absorption coefficients of Eu-complex and Eu-complex-DNA. [Eu-complex]$_0$ and [DNA]$_0$ are the initial concentration of Eu-complex and DNA, respectively. Figure 11 depicts a plot of 1/ΔA as a function of 1/[DNA] for Eu-complex-DNA system. Good linear correlations were obtained, confirming the formation of a 1:1 Eu-complex: DNA. From the intercept and slope value of this plot, K is evaluated at room temperature (25 °C).

The association constant at room temperature was determined to be $2.5\times10^4\pm100$ M^{-1} through the regression fit with correlation coefficient about 0.999.

The effect of DNA concentrations on the fluorescence intensity of Eu (III) exhibited a pronounced change in emission intensity as shown in (Fig. 12). The fluorescence intensity of Eu(III) in the complex enhanced remarkably with an increased DNA concentration.

The changes induced in the fluorescence intensity of Eu (III) complex in the presence of different DNA concentrations can be analyzed to obtain the binding constant and stoichiometry of the Eu(III)–(9-ACA)$_2$–DNA system according to the following equation [48]:

$$\log\left[\frac{F_0 - F}{F}\right] = \log K + n\log[Q] \quad (2)$$

where K and n are the binding constant and the number of binding sites, respectively. The Plot of log [(F_0–F)/F] versus log [Q] at room temperature gave a straight line (Fig. 13). The slope of such curve is equal to n while the

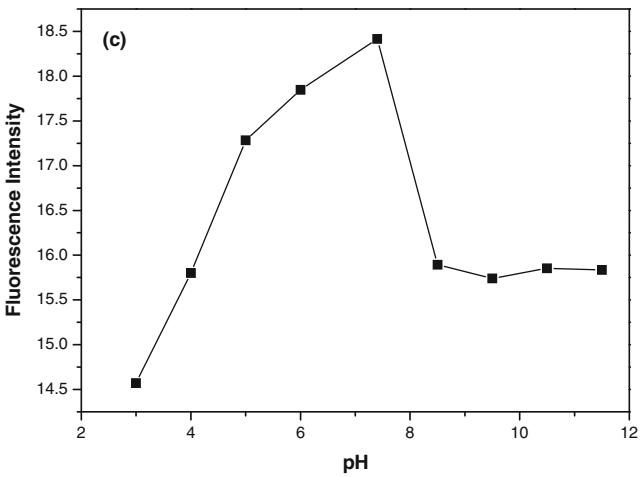

Fig. 9 Dependence of relative fluorescence intensity of Eu(III)–(9-ACA)$_2$–DNA complex on the pH values

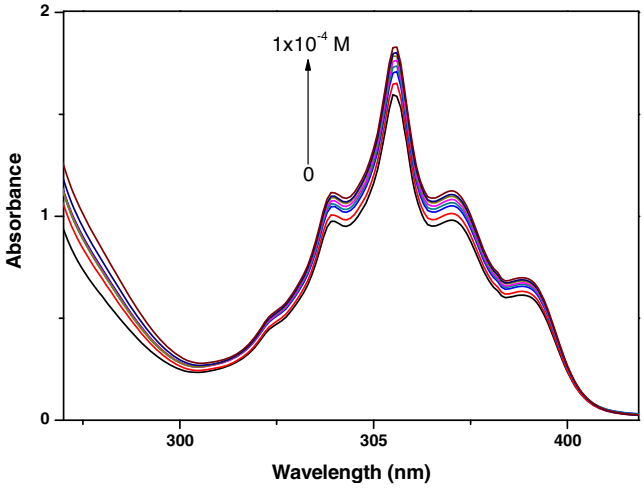

Fig. 10 Absorption spectra of Eu(III) complex in the absence and the presence of increasing amounts of CT-DNA. Arrows show the absorbance changes upon increasing CT-DNA concentration

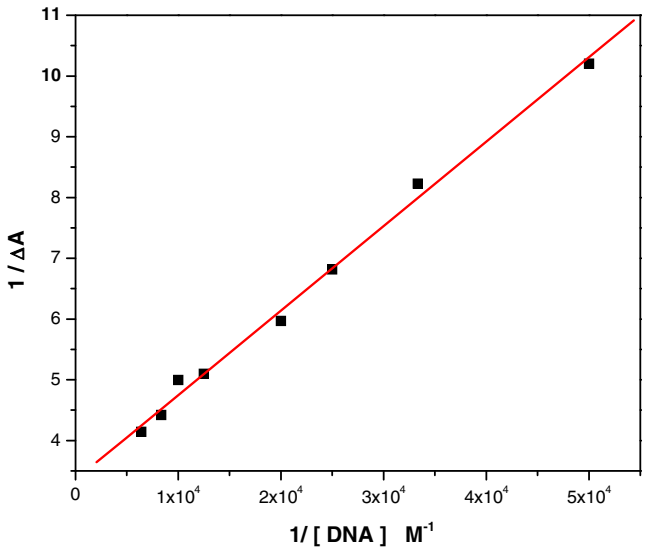

Fig. 11 Double reciprocal plot (Benesi-Hildebrand plot) for the effect of DNA concentration on the absorption of Eu(III)-(9-ACA)$_2$ complex at room temperature

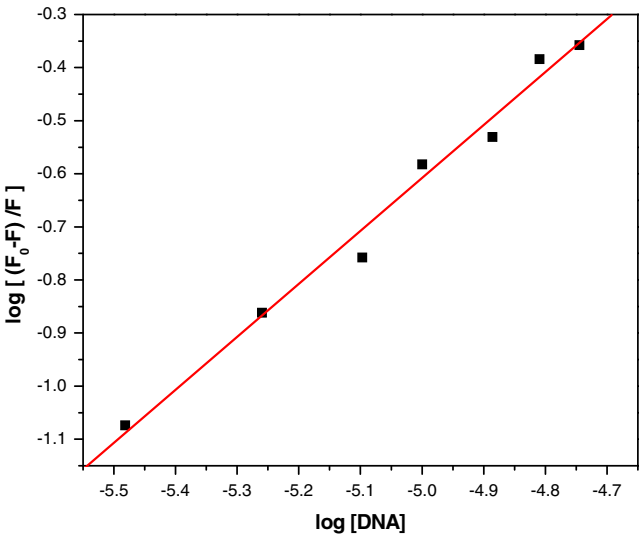

Fig. 13 Double logarithm plot of the fluorescence titration data of Eu (III)-(9-ACA)$_2$ complex with different concentration of DNA at room temperature

intercept to log K. The values of n approximately equal to 1, indicating that there is one binding site in Eu(lll) -9-ACA for DNA. The association constant at room temperature was determined to be $2.41 \cdot 10^4 \pm 100\ M^{-1}$ through the regression fit, which is very comparable to that calculated from the absorption titration with correlation coefficient of 0.9999. It was observed that the negative sign for free energy ΔG (25.1 Kcal/mol) means that the interaction process of Eu(9-ACA)$_2$ and DNA is spontaneous.

Calibration Curve for DNA

The luminescence enhancement of the Eu(III)-(9-ACA)$_2$ complex was studied in different concentrations of DNA in a luminescence titration experiment. Calibration graphs for the DNA determination are shown in (Fig. 14). There was a good linear relationship between the fluorescence enhancement and DNA concentration. The linear ranges were 9–50 ng for DNA. The limit of detection (LOD) was given by the equation, $LOD = K\sigma/s$, where K is a numerical factor chosen according to the confidence level desired, σ is the standard deviation of the blank measurements (n=7) and s is the sensitivity of the calibration graph. It can be seen that the detection limit is 5 ng $mL^{-1}$for DNA with the correlation coefficients 0.9999.

The use of Eu(III) chelates as luminescent indicators, rather than conventional fluorophores, can enable highly

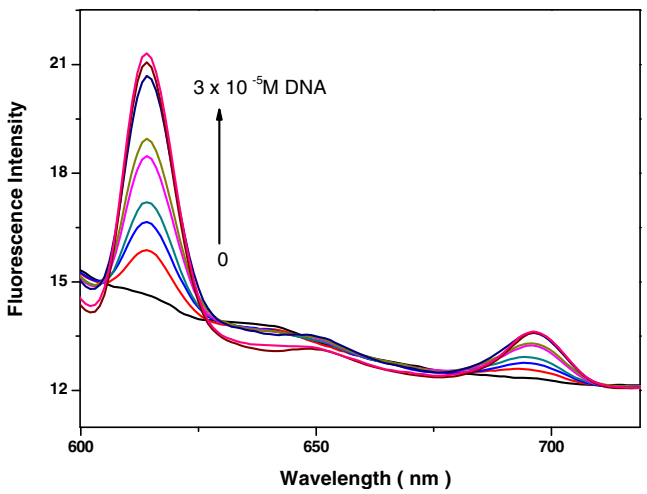

Fig. 12 Fluorescence spectra of Eu-complex in different concentration of DNA. [Eu-complex]=2×10^{-5} M; [DNA]/(10^{-5} M); 0, 2, 4, 6, 10

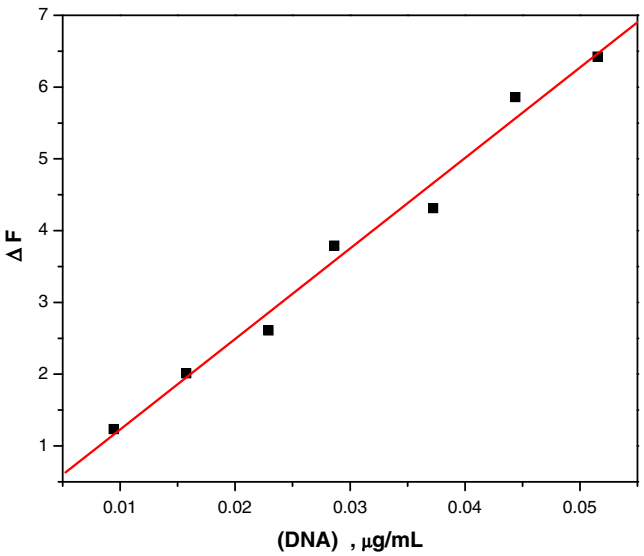

Fig. 14 Calibration curve of DNA: effect of DNA concentration on the fluorescence intensity of Eu(III)-(ACA)$_2$ at 615 nm

Table 3 Common luminescence probes for nucleic acid determination

DNA	Nucleic cid	LOD ng mL^{-1}	References
Ethidium bromide	nDNA	10	[52]
Hoechst 33258	nDNA	10	[53]
Methylene blue	nDNA	28	[54]
Vitamin K3	nDNA, RNA	10, 26	[55]
La-8-hydroxyquinoline	ctDNA, fsRNA	76, 68	[56]
Al-8-hydroxyquinoline	ctDNA, fsRNA	24, 13	[57]
Tb-1,10-phenanthroline	dDNA, RNA	100	[58]
Tb-BPMPHD-CTMAB	nDNA	9	[59]
Eu-Benzoylacetone–CTMAB	DNA, RNA	0.33, 0.99	[60]
Eu-oxytetracycline	nDNA	11	[61]
PicoGreen	dsDNA	0,25	[62]

sensitive detection due to their specific properties. In particular, the large Stokes' shift of lanthanide chelates (mostly $Eu^{3+}$and Tb^{3+}) easily permits selection of the chelate specific emission from scattered excitation light, even with filters. The narrow emission bands allow efficient separation of several luminescence signals in multicolor assays. Further, the very long luminescence life time permits gated detection on a micro- to millisecond timescale, to avoid typical short-lived non-specific background signals [49, 50]. In these systems, intense ion luminescence originates from the intramolecular energy transfer from the excited triplet-state of the ligand to the emitting level of the lanthanide (antenna effect) [51].

Table 3 gives some probes for determination of nucleic acids [52–62]. Eu(III)-$(ACA)_2$ complex is more sensitive than ethidium bromide which is carcinogenic.

Influence of Some Metal Ions and Foreign Substances on the Binding Between Eu-(9-ACA)$_2$ and DNA

There are a lot of coexisting substances which may lead to foreign interference with DNA in physiological environment.In order to investigate the effect of possible interference during our method certain concentrations of some ions and several kinds of amino acids were added to the Eu-(9-$ACA)_2$–DNA system and the changes of fluorescence intensity were recorded. The results are given in Table 4. Some metal ions, such as Al^{3+}, Pb^{2+}, Ni^{2+}, Mg^{2+} and Co^{2+} yielded slight interferences in DNA detection. Potential interferences of calcium and magnesium ions at the 10–50 micromolar concentration level were considered - and shown to have little effect on the fluorescence intensity. We have carried out interference study in the presence of more realistic concentrations of calcium and magnesium(in the milimolar range) to mimic the physiological levels of these ions. No pronounced increase in their interference has been observed which my support the possibility of using the method in physiological medium. The complete investigation and microbiological studies and the effect of our complex on different cancer lines are now under consideration in our lab with the aim to try to discover a new drug. The interferences of other coexisting substances were negligible. We studied the effect of cofluorescence of Gadolinium and Terbium on the fluorescence intensity of

Table 4 Tolerable concentration of coexisting substances in the Eu(III)-(9-$ACA)_2$ complex (10 μM) with DNA (10.0 μM)

Coexisting substances	concentration (μM)	Change of luminescence intensity (%)	Coexisting substances	concentration (μM)	Change of luminescence intensity (%)
Ca^{2+}	50	−0.1	NH_4^+	100	+1.0
Cd^{2+}	50	−0.1	Ni^{2+}	100	+3.4
Co^{2+}	100	−0.2	Pb^{2+}	100	−2.0
Cu^{2+}	100	−0.5	Mn^{2+}	50	−0.5
K^+	100	−2.0	Glucose	100	−0.1
Al^{3+}	75	−1.0	Tryptophan	50	−0.4
Mg^{2+}	50	−2.0	Terbium	50	−0.1
Po_4^-	50	−0.6	Gadalunium	50	−0.1
Na^+	75	−0.5			

(−) quenching; (+) enhancing

Eu(III)-(9-ACA)$_2$-DNA system. There is no pronounced effect on the fluorescence intensity. Interference of coexisting substances is investigated according to a procedure which includes the addition of these substances to the standard samples containing 10 μM DNA. The results are listed in Table 4. The data indicate that most of the metal ions have no effect on the method at the concentration of 50 to 100 μM, i.e., this method had high tolerance limits.

Conclusions

The newly synthesized Eu(III)-(9-ACA)$_2$ complex may be considered as a new fluorescencent probe for detection of DNA. This new probe has been applied to CT-DNA detection and the experimental results suggested that this method is simple, rapid, sensitive and stable.

The Eu(III) is coordinated through the hydroxylic oxygen atoms of acridine carboxylic group via deprotonation. The binding of the ligand to metal ion is confirmed by the analytical, FTIR, mass, ^{1}H-NMR spectra, and thermal analysis. To evaluate its potential pharmaceutical activities, the DNA-binding property was investigated by UV–vis absorption and fluorescence spectra. The Eu(III)-(9-ACA)$_2$-complex displays a low fluorescence intensity for Eu(III), but on binding to DNA the luminescence intensity increases. The changes in the fluorescence intensity have been used for the quantitative determination of DNA over a large linear concentration range (9–50 ng mL^{-1}) with LOD of 5 ng mL^{-1}. Hyperchromism was observed from the absorption experiment and binding constants have been determined with using both fluorescence and absorption data. The experimental data confirmed the formation of 1:1 complexes of Eu(III)-(9-ACA)$_2$ with DNA and the binding processes were spontaneous.

References

1. Erkkila KE, Odom DT, Barton JK (1999) Recognition and reaction of metallointercalators with DNA. Chem Rev 99:2777–2796
2. Jakupec MA, Unfried P, Keppler BK (2005) Pharmacological properties of cerium compound. Rev Physiol Biochem Pharmacol 153:101–11
3. Di GC, De MM, Chiron J, Delmas F (2005) Synthesis and antileishmanial activities of 4,5-di-substituted acridines as compared to their 4-mono-substituted homologues. Bioorg Med Chem 13:5560–5568
4. Rauf S, Gooding J, Akhtar K, Ghauri M, Rahman M, Anwar M, Khalid A (2005) Electrochemical approach of anticancerdrugs–DNA interaction. J Pharm Biomed Anal 37:205–217
5. Gamage S, Tepsiri N, Wilairat P, Wojcik S, Figgit D, Ralph R, Denny W (1994) Synthesis and in vitro evaluation of 9-anilino-3,6-diaminoacridines active against a multidrug-resistant strain of the malaria parasite plasmodium falciparum. J Med Chem 37:1486–1494
6. Gamage SA, Figgit DP, Wojcik SJ, Ralph RK, Ransijn A, Mauel J, Yardly V, Snowdon D, Croft SL, Denny WA (1997) Structure –activity relationships for the antileishmanial and antitrypanosomal activities of 1'-substituted 9-anilinoacridines. J Med Chem 40:2634–2642
7. Mauel J, Denny WA, Gamage SA, Ransijn A, Wojcik SL, Figgit DP, Ralph R (1993) 9-anilinoacridines as potential antileishmanial agents. Antimicrob Agents Chemother 37:991–996
8. Rewcastle GW, Atwell GJ, Chambers D, Baguley BC, Denny WA (1986) Potential antitumor agents. 46. Structure-activity relationships for acridine monosubstituted derivatives of the antitumor agent N-[2-(dimethylamino)ethyl]-9-aminoacridine-4-carboxamide. J Med Chem 29:472–477
9. Li J, Wei Y, Guo L, Zhang C, Jiao Y, Shuang S, Dong C (2008) Study on spectroscopic characterization of Cu porphyrin/Co porphyrin and their interactions with ctDNA. Talanta 76:34–39
10. Ni Y, Lin D, Kokot S (2008) Synchronous fluorescence and UV–vis spectroscopic studies of interactions between the tetracycline antibiotic, aluminium ions and DNA with the aid of the Methylene Blue dye probe. Anal Chim Acta 606:19–25
11. Araya F, Huchet G, McGroarty I, Skellern GS, Waigh RD (2007) Capillary electrophoresis for studying drug–DNA interactions. Methods 42:141–149
12. Sandstrom K, Warmlander S, Leijon M, Graslund A (2003) 1H NMR studies ofselective interactions of norfloxacin with double-stranded DNA. Biochem Biophys Res Commun 304:55–59
13. Wang L, Lin L, Ye B (2006) Electrochemical studies of the interaction of the anticancer herbal drug emodin with DNA. J Pharm Biomed Anal 42:625–629
14. Atwell GJ, Rewcastle GW, Baguley BC, Denny WA (1987) Potential antitumor agents. 50. In vivo solid-tumor activity of derivatives of N-[2-(dimethylamino) ethyl]acridine-4-carboxamide. J Med Chem 30:664–669
15. Graves DE, Velea LM (2000) Intercalative binding of small molecules to nucleic acids. Curr Org Chem 4:915–929
16. Atwell GJ, Cain BF, Baguley BC, Finlay GJ, Denny WA (1984) Potential antitumor agents. Part 43. Synthesis and biological activity of dibasic 9-aminoacridine-4-carboxamides, a new class of antitumor agent. J Med Chem 27:1481–1485
17. Bi S, Zhang H, Qiao C, Sun Y, Liu C (2008) Studies of interaction of emodin and DNA in the presence of ethidium bromide by spectroscopic method. Spectrochim Acta 69:123–129
18. Sabolova D, Kozurkova M, Kristian P, Danihel I, Podhradsky D, Imrich J (2006) Determination of the binding affinities of plasmid DNA using fluorescent intercalators possessing an acridine skeletonInt. J Biol Macromol 38:94–98
19. Liu R, Yang J, Sun C, Li L, Wu X, Li Z, Qi C (2003) Study of the interaction of nucleic acids with acridine orange-CTMAB and determination of nucleic acids at nanogram levels based on the enhancement of resonance light scattering. Chem Phys Lett 376:108–115
20. Liu SP, Chen S, Liu ZF, Hu XL, Shan T (2005) Resonance Rayleigh scattering spectra of interaction of sodium carboxymethylcellulose with cationic acridine dyes and their analytical applications. Anal Chim Acta 535:169–175
21. Wang M, Yang J, Wu X, Huang F (2000) Study of the interaction of nucleic acids with acridine red and CTMAB by a resonance light scattering technique and determination of nucleic acids at nanogram levels. Anal Chim Acta 422:151–158
22. Azab HA, Anwar ZM, Ahmed RG (2010) Pyrimidine and purine mononucleotid es recognition by trivalent lanthanide complexes with N-acetyl amino acids. J Chem Eng Data 55:459–475
23. Azab HA, El-Korashy SA, Anwar ZM, Hussein BHM, Khairy GM (2010) Synthesis and fluorescence properties of Eu-anthracene-9-carboxylic acid towards Nacetylamino acids and

nucleotides in different solvents. Spectrochim Acta Part A 75:21–27
24. Azab HA, Abd El-Gwad II, Kamel RM (2009) Ternary complexes formed by the fluorescent probe Eu(III)-anthracene-9-carboxylic acid with pyrimidine and purine nucleobases. J Chem Eng Data 54:3069–3078
25. Azab HA, El-Korashy SA, Anwar ZM, Hussein BHM, Khairy GM (2010) Eu(lll)-anthracene-9-carboxylic acid as a responsive luminescent bioprobe and its electroanalytical interactions with N-acetyl amino acids, nucleotides and DNA. J Chem Eng Data 55:3130–3141
26. Azab HA, Al-Deyab SS, Anwar ZM, Gharib RA (2011) Fluorescence and electrochemical probing of N-acetylamino acids, nucleotides and DNA by Eu(III)—bathophenanthroline complex. J Chem Eng Data 56:833–849
27. Azab HA, Al-Deyab SS, Anwar ZM, Kamel RM (2011) Potentiometric, electrochemical and fluorescence study of the coordination properties of the monomeric and dimeric complexes of Eu(III) with Nucleobases and PIPES. J Chem Eng Data 56:1960–1969
28. Azab HA, Al-Deyab SS, Anwar ZM, Abd El-Gawad II, Kamel RM (2011) Comparison of the coordination tendency of amino acids, nucleobases or mononucleotides towards the monomeric and dimeric lanthanide complexes with biologically important compounds. J Chem Eng Data 56:2613–2625
29. Ali R, Saleh SM, Meier RJ, Azab HA, Abdelgawad II, Wolfbeis OS (2010) Upconverting nanoparticle based optical sensor for carbon dioxide. Sensors and Actuators B 150:126–131
30. Liu XW, Li J, Li H, Zheng KC, Chao H, Ji LN (2005) Synthesis, characterization, DNA-binding and photocleavage of complexes [Ru(phen)2(6-OH-dppz)]2+ and [Ru(phen)2(6-NO2-dppz)]2+. J Inorg Biochem 99:2372–2380
31. Kumar CV, Asuncion EH (1993) DNA binding studies and site selective fluorescence sensitization of an anthryl probe. J Am Chem Soc 115:8547–8553
32. Welcher FJ (1965) The analytical uses of ethylene diaminetetraacetic acid. D. Von Nostrand Co., Inc., Princeton
33. Hart FA, Laming FP (1964) Complexes of 1,10-phenanthroline with lanthanide chlorides and thiocyanates. J Inorg Nucl Chem 26:579–585
34. Wang Y, Wang Y, Yang ZY (2007) Synthesis, characterization and DNA-binding studies of 2-carboxybenzaldehydeisonicotinoylhydrazone and its La(III), Sm(III) and Eu(III) complexes. Spectrochim Acta A 66:329–334
35. Nakamoto K (1986) Infrared and Raman spectra of inorganic and coordination compounds. Wiley, New York
36. Deacon GB, Phillips RJ (1980) Relationships between the carbon-oxygen stretching frequencies of carboxylato complexes and the type of carboxylate coordination. Coord Chem Rev 33:227–250
37. Ryu CK, Endicott JF (1988) Synthesis, spectroscopy, and photophysical behavior of mixed-ligand mono- and bis(polypyridyl) chromium(III) complexes. Examples of efficient, thermally activated excited-state relaxation without back intersystem crossing. Inorg Chem 27:2203–2214
38. Choppin GR, Peterman DR (1998) Applications of lanthanide luminescence spectroscopy to solution studies of coordination chemistry. Coord Chem Rev 174:283–299
39. Fischer G, Naaman R (1976) Near Resonance vibronic coupling. Isoquinoline J Chem Phys 12:367–379
40. Schulman SG (1977) Fluorescence and phosphorescence spectroscopy: Physicochemical principles and practice. Pergamon, New York, p 60
41. Pasternack RF, Gibbs EJ, Villafranca JJ (1983) Interactions of porphyrins with nucleic acids. Biochemistry 22:2406–2414
42. Ling LS, He ZK, Chen F, Chen F, Zeng YE (2003) Single-mismatch detection using nucleic acid molecular 'light switch'. Talanta 59:269–275
43. Kumar CV, Barton JK, Turro NJ (1985) Photophysics of ruthenium complexes bound to double helical DNA. J Am Chem Soc 107:5518–5523
44. Xu H, Zheng KC, Chen Y, Li YZ, Lin LJ, Li H, Zhang PX, Ji LN (2003) Effects of ligand planarity on the interaction of polypyridyl Ru(II) complexes with DNA. Dalton Trans 11:2260–2268
45. Hirohama T, Kuranuki Y, Ebina E, Sugizaki T, Arii H, Chikira M, Selvi PT, Palaniandavar M (2005) Copper(II) complexes of 1,10-phenanthroline-derived ligands: Studies on DNA binding properties and nuclease activity. J Inorg Biochem 99:1205–1219
46. Barton JK, Danishefsky A, Goldberg J (1984) Tris (phenanthroline) ruthenium(II): stereoselectivity in binding to DNA. J Am Chem Soc 106:2172–2176
47. Benesi HA, Hildebrand JH (1949) A spectrophotometric investigation of the interaction of iodine with aromatic hydrocarbons. J Am Chem Soc 71:2703–2707
48. Kang J, Liu Y, Xie M, Li S, Jiang M, Wang Y (2004) Interactions of human serum albumin with chlorogenic acid and ferulic acid. Biochim Biophys Acta 1674:205–214
49. Elbanovski M, Makowska B (1996) The lanthanides as luminescent probes in investigations of biochemical systems. J Photochem Photobiol A 99:85
50. Gudgin Dickson EF, Pollak A, Diamandis EP (1995) Time-resolved detection of lanthanide luminescence for ultrasensitive bioanalytical assays. J Photochem Photobiol B 27:3
51. Lis S, Elbanowski M, Makowska B, Hnatejko Z (2002) Energy transfer in solution of lanthanide complexes. Photobiology A 150:233
52. Lepecq JB, Paoletti C (1966) A new fluorometric method for RNA and DNA determination. Anal Biochem 17:100–107
53. Labara C, Paigen K (1980) A simple, rapid, and sensitive DNA assay procedure. Anal Biochem 102:344–352
54. Li WY, Xu JG, Guo XQ, Zhu QZ, Zhao YB (1997) A novel fluorometric method for DNA and RNA determination. Anal Lett 30:527–536
55. Li WY, Xu JG, Guo XQ, Zhu QZ, Zhao YB (1997) Application of vitamin K3 as a photochemical fluorescence probe in the determination of nucleic acids. 30:245–257
56. Huang CZ, Li KA, Tong SY (1996) Fluorescent complexes of nucleic acids/8- hydroxyqulnollne/lanthanum(III) and the fluorometry of nucleic acids. Anal Lett 29:1705–1717
57. Huang CZ, Li KA, Tong SY (1997) Spectrofluorimetric determination of nucleic acids with aluminum(III)/8-hydroxyquinoline complex. Anal Lett 30:1305–1319
58. Ci YX, Li YZ, Chang WB (1991) Fluorescence reaction of terbium(III) with nucleic acids in the presence of phenanthroline. Anal Chim Acta 248:589–594
59. Wu X, Yang J, Huang F, Wang M, Sun L, Xu G (1999) Study of the reaction between nucleic acids and Tb-BPMPHD-CTMAB complex and its analytical application. Anal Lett 32:2417–2425
60. Wu X, Guo Ch, Yang J, Wang M, Chen Y, Liu J (2005) The sensitive determination of nucleic acids using fluorescence enhancement of Eu3+−benzoylacetone-cetyltrimethylammonium bromide-nucleic acid system. J Fluorescence 15:655–660
61. Liu R, Yang J, Wu X (2002) Study of the interaction between nucleic acid and oxytetracycline–Eu3+ and its analytical application. J Luminescence 96:201–209
62. Haugland RP (Ed.) (2003) Handbook of Fluorescent Probes and Research Products. Molecular Probes 9:301–304